Shape dependence of resonant energy transfer between semiconductor nanocrystals

Joshua Schrier* and Lin-Wang Wang

Computational Research Division, Lawrence Berkeley National Laboratory, Berkeley, California 94720 USA

We theoretically study the energy transfer between semiconductor nanocrystal dots and rods of CdSe using a semiempirical pseudopotential method (SEPM) description of the electronic structure of the nanocrystals, followed by evaluation of the Coulombic contribution to the energy transfer evaluated using the transition density cube (TDC) method. Our results are compared to the dipole-dipole theory of Förster to characterize the effects of nanocrystal shape, distance, and orientation. For the distances typical of nanorod solids, we find that the dipole-dipole theory underestimates the coupling between linearly oriented nanorods by as much as a factor of two, and overestimates the coupling between parallel nanorods by as much as a factor of three.

I. INTRODUCTION

A number of experimental studies of resonant energy transfer between colloidal semiconductor nanocrystals have been undertaken.[1–7] In addition to fundamental interest, the resonant energy transfer-based quenching of quantum-dot fluorophores has found widespread use in experimental molecular biology.[8] The theoretical treatments of these phenomena typically have utilized a dipole-dipole approximation to estimate the coupling between the nanocrystals,[9–11] however, as noted by Krueger *et al.*,[12,13] the asymmetric shape and/or large spatial extent of the transition densities can make this type of approximation invalid. To date, the efforts to go beyond the dipole approximation description of energy transfer between nanocrystals have been limited to effective mass description by Govorov,[14] and very recently a semi-empirical tight-binding approach by Allan and Delerue.[15] However, both of these have only considered spherical nanocrystals. Thus, the goal of this paper is to utilize the semiempirical pseudopotential method (SEPM) to study the coupling between nanocrystalline CdSe quantum dots and rods, to determine to what extent, if any, the dipole-dipole approximation fails for rod-shaped nanocrystals.

II. THEORY

The calculation of the resonant energy transfer uses the transition density cube (TDC) method of Krueger *et al.*[12,13] In the weak-coupling limit, the exciton transfer rate is given as

$$k = \frac{1}{\hbar^2 c}|V|^2 J, \tag{1}$$

where V is the electronic coupling and J is the spectral overlap between the donor and acceptor spectra. The dependence of spectral overlap, J, on the size difference of the two quantum dots and the temperature has been studied previously.[2,6] Here, we will focus on the electron coupling term, V. To simplify our treatment, so as to focus more clearly upon the shape and orientation dependence of the of the resonant energy transfer, we consider coupling between two identical nanocrystals, occurring at low temperature so that we may consider the exciton to consist only of the single lowest-energy electron level (CBM) and single highest-energy hole level (VBM). Within the Förster theory, the electronic coupling is then assumed to be the result of Coulombic contributions between singlet states on the donor and acceptor. In the widely used dipole-dipole approximation, this is simply

$$V^{dd} = \frac{1}{4\pi\epsilon_0}\kappa\frac{|\mu_D||\mu_A|}{R^3}, \tag{2}$$

where μ is the transition dipole matrix element between the ground and excited state on either the donor (D) or acceptor (A), $\kappa = \hat{\boldsymbol{r}}_D\cdot\hat{\boldsymbol{r}}_A - 3(\hat{\boldsymbol{r}}_D\cdot\hat{\boldsymbol{R}})(\hat{\boldsymbol{r}}_A\cdot\hat{\boldsymbol{R}})$, where $\hat{\boldsymbol{R}}$ is the unit vector connecting the centers of the transition moments and $\hat{\boldsymbol{r}}_D, \hat{\boldsymbol{r}}_A$ are unit vectors in the directions of the donor and acceptor transition dipoles. It is well known that Eq.(2) is only valid for large dipole-dipole distances and neglects the higher multipole interactions. However, in nanocrystal assemblies, such as quantum-dot solids[16,17], the interparticle distance is comparable to the size of the nanocrystal itself. Thus it is extremely interesting to study the validity of Eq.(2). The previous theoretical treatment of spherical quantum dots found that the distance-scaling relation of Eq.(2) was retained even at close distances.[15] Here we study nanorod interactions, which have more complicated behavior (*vide infra*). The full Coulombic interaction is calculated within the TDC method by use of the transition density formalism of McWeeny.[18] For the single electron-single hole case described above, the transition density is defined as

$$M_N(\boldsymbol{r}) = \psi_{N,h}(\boldsymbol{r})\psi^*_{N,e}(\boldsymbol{r}) \tag{3}$$

for the donor ($N = D$) and acceptor ($N = A$) nanoparticles. The wavefunctions for the electron, $\psi_{N,e}$,and hole, $\Psi_{N,h}$, are calculated by the SEPM method and described on a real-space grid. The SEPM approach, and its application to CdSe nanorods, has been described previously.[19] The integral over space of M_N can be slightly different than zero (in

our calculations it was typically 10^{-4} e) due to numerical errors, this is compensated by adding a small equivalent amount of charge to M_N to make the integrated charge zero. Then, the Coulombic coupling may be expressed as

$$V^{coul} = \int \mathrm{d}\boldsymbol{r_1}\mathrm{d}\boldsymbol{r_2}\frac{M_D(\boldsymbol{r_1})M_A(\boldsymbol{r_2})}{4\pi\epsilon|\boldsymbol{r_1}-\boldsymbol{r_2}|}. \tag{4}$$

Moreover, since the Cartesian components, α, of the transition dipole can be expressed as

$$\mu_\alpha = \int \mathrm{d}\boldsymbol{r_1} r_\alpha M_N(\boldsymbol{r_1}), \tag{5}$$

the same transition densities can be used in the evaluation of Eq.(2), allowing a direct comparison against Eq.(4). In order to better illustrate the differences between the full Coulombic coupling and the dipole approximation, we will plot the ratio $|V^{coul}|^2/|V^{dd}|^2$.

At this point we compare the current method to that of Allan and Delerue.[15] First, in their calculation they include the role of the dielectric screening, and find that this does not change the scaling behavior of the Förster rate, even though for a particular dielectric constant (both inside the respective nanocrystals and in the surrounding matrix), this can have an effect on the actual value of the transfer coupling. By considering the ratio between V^{coul} and V^{dd}, we avoid the explicit choice of dielectric constant, and thus focus on the shape and orientation dependence only. Second, in their work, the matrix elements of V were calculated based on approximating the total transition density as localized atomic point transition charges. This type of approach can be derived as an approximation to Eq.(4) when the atomic transition charges are fit to an electrostatic potential,[20] although the work of Allan and Delerue is closest to the zero-differential overlap (ZDO) type model of Hennebicq *et al.*[21] Third, we do not treat the effect of temperature on the donor state (by means of a Boltzmann distribution as in their work), although this can be included in the evaluation of Eq.(4). On the other hand, this does not encompass all of the effects of finite temperature on the energy transfer rate, such as the combined temperature and size dependence of the nanocrystal band gap itself (e.g., as in recent first principles calculations of Si nanocrystals by Franceschetti[22]), or the temperature and size dependence of the emission and absorption spectra (e.g., as studied in recent single CdSe nanocrystal experiments by Liptay *et al.*[23]). While all of the previous studies deal with spherical quantum dots, our study is focused on the shape and orientation dependence of the FRET.

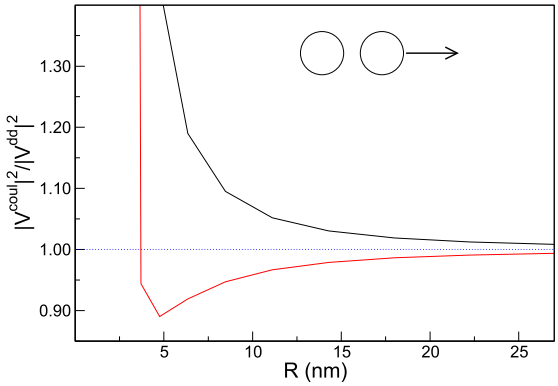

FIG. 1: (Color online) Ratio between the full Coulombic (V^{coul}) and dipole-dipole (V^{dipole}) coupling terms, as a function of the distance between the two spherical 2-nm diameter CdSe nanocrystals. The black and red lines indicate cases where the two quantum dots are displaced along and perpendicular to the wurtzite axis, respectively, and in both cases the wurtzite axes of the two nanocrystals are parallel to each other.

III. RESULTS AND DISCUSSION

A. Dots

To begin our study, we examined the case of spherical 2nm-diameter CdSe nanocrystals, shown in Figure 1. This will allow us to compare our calculations to the previous studies. At very small distances, e.g., less than 4 nm center-to-center, the dipole-dipole expression substantially underestimates the full Coulombic coupling. As expected, at large separations, Eq.(4) and Eq.(2) are identical. This is consistent with the behavior of 1.5 nm diameter spherical InAs and 1.36 nm diameter spherical Si nanocrystals in the study of Allan and Delerue,[15] where the only deviations from the R^{-6} scaling of the dipole-dipole expression occurred at small inter-dot distances.

B. Rods

In rod-shaped nanocrystals, the wavefunction is extended along the length of the rod. As a result, the transition densities, shown in Figure 2 are not well described by the simple point-dipole approximation. As a concrete example, we examine the case of two identical 1.7 nm diameter × 5nm long CdSe wurtzite nanorods, where the long axis is along the *c*-axis of the wurtzite structure. Below we consider linear, parallel, and perpendicular alignments of the rods with respect to each other, so as to illustrate some of the general effects.

We first examine the case of linearly oriented nanorods. Since the wurtzite crystal structure lacks inversion symme-

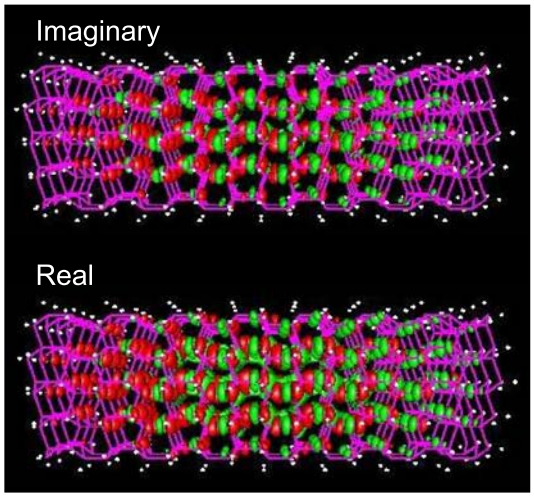

FIG. 2: (Color online) Transition density, $M_N(\boldsymbol{r})$ (Eq.(3))for the 1.7 nm diameter $\times$ 5nm long CdSe wurtzite nanorod studied in this work. Red and green contours indicate positive and negative signs, respectively, for both the real and imaginary parts.

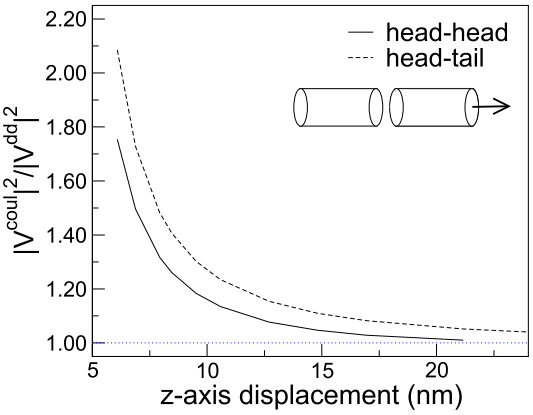

FIG. 3: (Color online) Ratio of the full Coulombic (V^{coul}) and dipole-dipole (V^{dd}) electronic coupling between two linearly-oriented CdSe nanorods as a function of center-to-center distance. The solid and dashed lines show the results for head-head (‘(wurtzite c-axes oriented antiparallel to each other) and head-tail (wurtzite c-axes oriented parallel to each other) orientations, respectively. The inset depicts the relative motion of the nanorods being considered.

try, there are two possible orientations of these nanorods. Either the wurtzite c-axes of the two rods can be oriented antiparallel with respect to each other (pointing the nanocrystals “head-head”) or parallel to each other (pointing the nanocrystals “head-tail”). A head-tail arrangement has been hypothesized as an explanation for self-assembly of CdSe nanorods.[24] Figure 3 shows that the dipole-dipole approximation underestimates the electronic coupling between the nanorods, at all separations, although the two expressions become equal at large distances.

Next we examine the case of parallel nanorods. As in the linear case discussed above, the rods may either be oriented

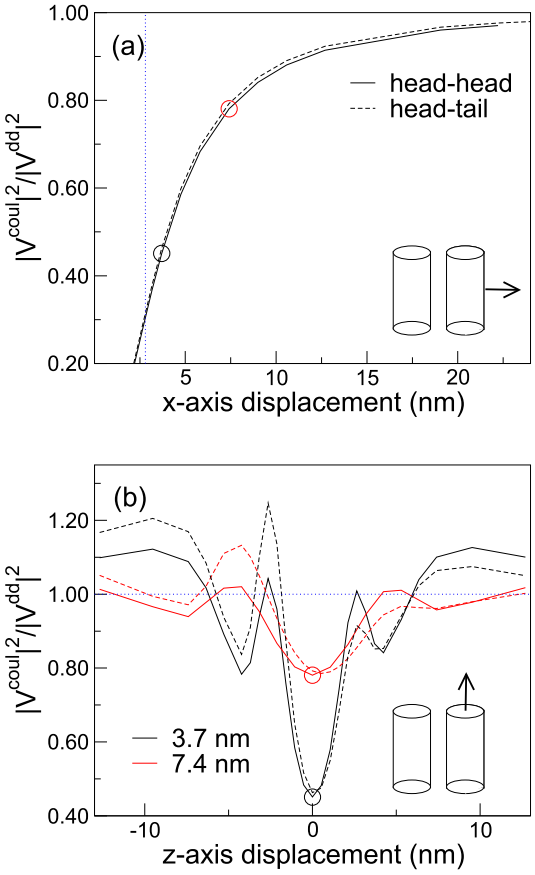

FIG. 4: (Color online) Electronic coupling between two parallel CdSe nanorods. The insets depicts the relative motion of the nanorods being considered. In (b), 3.7 nm and 7.4 nm are the rod-rod distances when at zero z-axis displacement, with the black and red circles indicating reference points between plots (a) and (b). The vertical dotted line in (a) indicates the minimum distance between the nanorods, including a 1.1 nm inter-rod spacing due to the organic capping ligands.

head-head or head-tail, and self-assembled CdSe nanorod structures are hypothesized to have head-tail orientation in this direction.[24] In Figure 4a, we show the results for the case of moving the two rods apart in the direction perpendicular to the rod alignment. For all distances, the full Coulombic coupling is less than that predicted by the dipole-dipole approximation and asymptotically becomes equal to the dipole-dipole case at large distance. The behavior is similar for both the head-head and head-tail alignments. In both quantum dot[17] and nanorod[25] self-assembly experiments the inter-rod spacing is about 1.1 nm (twice the length of the surface capping ligands). The vertical dotted line in Figure 4a indicates the minimum allowed center-to-center distance (including the 1.1nm spacing due to ligands) of 2.8 nm, at which the distance the full-Coulombic contribution to the exciton transfer rate is just

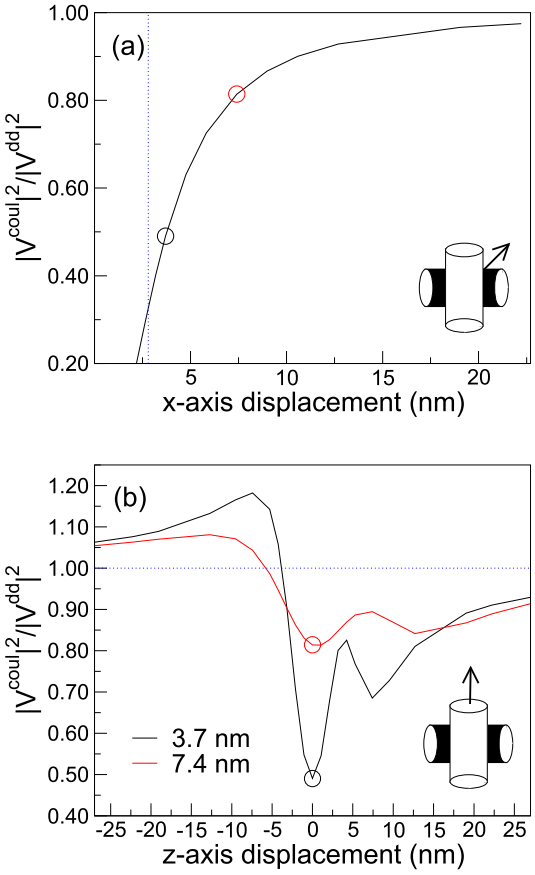

FIG. 5: (Color online) Electronic coupling between two perpendicularly oriented CdSe nanorods. In each case, the inset depicts the relative motion of the nanorods being considered, and the black and red circles indicate reference points which are the same in (a) and (b). The vertical dotted line in (a) indicates the minimum distance between the nanorods, including a 1.1 nm inter-rod spacing due to the organic capping ligands.

a third of the point-dipole model result. Thus, for the most experimentally relevant nearest-neighbor interparticle separation, the commonly used interpretation of experiment in terms of V^{dd} will substantially overestimate the actual exciton transfer rate. In Figure 4b, we consider two of these points, and consider the effect of displacing the rods as shown in the inset. For the head-head orientation (solid lines), the effect is symmetrical, and in both the 3.7-nm and 7.4-nm cases the correction factor oscillates about unity. In the head-tail orientation (dashed lines), the effect is unsymmetrical. In both cases the magnitude of the the deviation from unity is greatest when the z-axis separation is zero. These oscillations arise from the multipole effects neglected by the dipole-dipole model.

Finally, we consider the case of perpendicularly oriented nanorods. In this arrangement, the head-head or head-tail

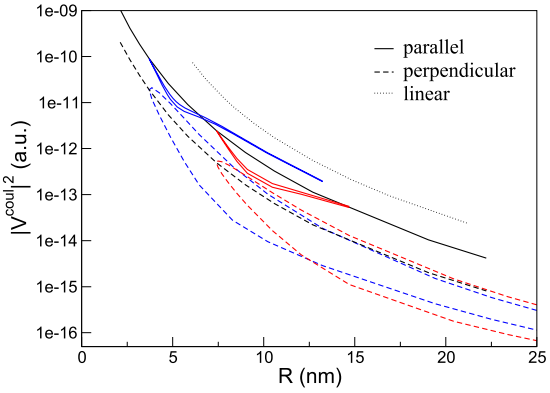

FIG. 6: (Color online) Coulombic electronic coupling between CdSe nanorods as a function of center-to-center distance, R. The dotted, solid, and dashed curves represent the linear, parallel, and perpendicular situations illustrated in the insets of Figs. 2, 3, 4, respectively. The blue and red curves show the 3.7nm and 7.4nm cases, respectively for the displacements shown in Figs. 3b and 4b. Note that there are two lines for each of the blue and red curves, representing the positive and negative z-axis displacements shown in Figs. 3b and 4b.

arrangements are equivalent, within an reflection in the plane of the page followed by rotation. As shown in Figure 5a, separation of the rods yields qualitatively similar results as discussed above in regards to Figure 4a. Next, choosing 3.7 nm and 7.4 nm as example distances, we can then see what happens as the rods are moved as shown in the inset of Figure 5b. The effects of this displacement are not symmetric, due to the lack of inversion symmetry in the wurtzite rods which distinguishes the orientation of the rods as seen in the plot of the transition density shown in Figure 2. However, this asymmetry is not well described by the simple dipole-dipole interaction model. Figure 5b illustrates the difference between having the "head" or "tail" of one rod closest to the center of the other rod. As in the case of the parallel rods, the magnitude of the correction factor is greatest when the z-axis separation is zero. It appears that there is a long-ranged contribution to the correction factor, up to z-axis displacements of 25 nm, although at those distances, the absolute value of V^{coul} is several orders of magnitude smaller than at close distances.

Finally, having compared the full Coulombic interaction against the dipole-dipole treatment, in Figure 6, we show the value of $|V^{coul}|^2$ for each of the linear, parallel, and perpendicular cases to see what circumstances give the largest coupling, and hence the fastest FRET transfer rates. The head-head and head-tail orientations are difficult to distinguish on the logarithmic scale, so for clarity only the head-tail orientations are shown. For this calculation we have taken $\epsilon = \epsilon_0$ both inside and outside the nanocrystal, for simplicity. The red and blue curves correspond to the two different x-axis displacements shown in Figs. 3b and 4b for the parallel and perpendicular cases, respectively. For the reasons discussed above, the positive and negative z-axis displacements for the parallel case have approximately

the same effect on the coupling, whereas in the perpendicular case the positive displacement gives the weaker coupling. Despite the much stronger coupling (at a given distance) for the linear case as opposed to the parallel case, the nanorods are much narrower than they are long, and so for the distances typical of close-packed nanorod solids, the nearest-neighbor exciton transfer occurs most quickly between parallel nanorods, and is about the same for perpendicular and linearly oriented rods.

IV. CONCLUSION

Previous experimental[2,3,7] and theoretical[14,15] treatments of resonant energy transfer between nanocrystals have considered only spherical structures, for which our calculations indicate that the full Coulombic interaction is well described by the point-dipole Förster model, in agreement with previous tight-binding calculations.[15] However, the energy transfer between nanocrystalline rods has not previously been studied, despite its applicability to studying, e.g., exciton migration in all-inorganic nanorod-based photovoltaic devices.[26] By examining the limiting cases of linear, parallel, and perpendicularly oriented nanorods, we observe more complicated behavior than predicted by the Förster model, which may be taken into account in the design and interpretation of future experiments. In particular, we find that for close-packed nanorod solids, the coupling between nearest-neighbor parallel nanorods can be as little as one-third of what would be predicted by the Förster model, which consequently reduces the estimates of exciton mobilities in these types of materials.

Acknowledgments

This work was supported by the U. S. Department of Energy under Contract No. DE-AC02-05CH11231, and used the resources of the National Energy Research Scientific Computing Center.

---

* Electronic address: jschrier@lbl.gov

[1] Mamedov, A. A.; Belov, A.; Giersig, M.; Mamedova, N. N.; Kotov, N. A. *J. Am. Chem. Soc.* **2001**, *123*, 7738.

[2] Crooker, S. A.; Hollingsworth, J. A.; Tretiak, S.; Klimov, V. I. *Phys. Rev. Lett.* **2002**, *89*, 186802.

[3] Franzl, T.; Klar, T. A.; Schietinger, S.; Rogach, A. L.; Feldmann, J. *Nano Lett.* **2004**, *4*, 1599.

[4] Koole, R.; Lijeroth, P.; de Mello Donegá, C.; Vanmaekelbergh, D.; Meijerink, A. *J. Am. Chem. Soc.* **2006**, *128*, 10436.

[5] Becker, K.; Lupton, J. M.; Müller, J.; Rogach, A. L.; Talapin, D. V.; Weller, H.; Feldmann, J. *Nature Mater.* **2006**, *5*, 777.

[6] Pons, T.; Medintz, I. L.; Sykora, M.; Mattoussi, H. *Phys. Rev. B* **2006**, *73*, 245302.

[7] Clark, S. W.; Harbold, J. M.; Wise, F. W. *J. Phys. Chem. C* **2007**, *111*, 7302.

[8] Clapp, A. R.; Medintz, I. L.; Mattoussi, H. *Chem. Phys. Chem.* **2006**, *7*, 47.

[9] Lovett, B. W.; Reina, J. H.; Nazir, A.; Briggs, G. A. D. *Phys. Rev. B* **2003**, *68*, 205319.

[10] Scholes, G. D.; Andrews, D. L. *Phys. Rev. B* **2005**, *72*, 125331.

[11] Hong, S.-K. *Physica E* **2005**, *28*, 66.

[12] Krueger, B. P.; Scholes, G. D.; Fleming, G. R. *J. Phys. Chem. B* **1998**, *102*, 5378.

[13] Scholes, G. D. *Annu. Rev. Phys. Chem.* **2003**, *54*, 57.

[14] Govorov, A. O. *Phys. Rev. B* **2005**, *71*, 155323.

[15] Allan, G.; Delerue, C. *Phys. Rev. B* **2007**, *75*, 195311.

[16] Kagan, C. R.; Murray, C. B.; Nirmal, M.; Bawendi, M. G. *Phys. Rev. Lett.* **1996**, *76*, 1517.

[17] Kagan, C. R.; Murray, C. B.; Bawendi, M. G. *Phys. Rev. B* **1996**, *54*, 8633.

[18] McWeeny, R. *Methods of Molecular Quantum Mechanics;* Academic Press: London, 2nd ed., 1992.

[19] Hu, J.; Wang, L.-W.; Li, L.-S.; Yang, W.; Alivisatos, A. P. *J. Phys. Chem. B* **2002**, *106*, 2447.

[20] Madjet, M. E.; Abdurahman, A.; Renger, T. *J. Phys. Chem. B* **2006**, *110*, 17268.

[21] Hennebicq, E.; Pourtois, G.; Scholes, G. D.; Herz, L. M.; Russell, D. M.; Silva, C.; Stayesh, S.; Grimsdale, A. C.; Müllen, K.; Brédas, J.-L.; Beljonne, D. *J. Am. Chem. Soc.* **2005**, *127*, 4744.

[22] Franceschetti, A. *Phys. Rev. B* **2007**, *76*, 161301.

[23] Liptay, T. J.; Marshall, L. F.; Rao, P. S.; Ram, R. J.; Bawendi, M. G. *Phys. Rev. B* **2007**, *76*, 155314.

[24] Talapin, D. V.; Shevchenko, E. V.; Murray, C. B.; Kornowski, A.; Förster, S.; Weller, H. *J. Am. Chem. Soc.* **2004**, *126*, 12984.

[25] Li, L.-S.; Alivisatos, A. P. *Adv. Mater.* **2003**, *15*, 408.

[26] Gur, I.; Fromer, N. A.; Geier, M. L.; Alivisatos, A. P. *Nature* **2005**, *310*, 462.